Astron. Astrophys. 333, 13–16 (1998)

ASTRONOMY AND ASTROPHYSICS

Localised neutral hydrogen absorption towards the radio jet of Markarian 6

J.F. Gallimore[1], **A.J. Holloway**[2], **A. Pedlar**[3], **and C.G. Mundell**[3]

[1] Max-Planck-Institut für extraterrestrische Physik, Postfach 1603, D-85740 Garching b. München, Germany
(e-mail: jfg@hethp.mpe-garching.mpg.de)
[2] Department of Physics and Astronomy, University of Manchester, Schuster Laboratory, Oxford Road, Manchester M13 9PL, UK
[3] Nuffield Radio Astronomy Laboratories, University of Manchester, Jodrell Bank, Macclesfield, Cheshire SK11 9DL, UK

Received 12 September 1997 / Accepted 10 November 1997

Abstract. We present $\sim 0\farcs15$ (56 pc) resolution MERLIN observations of neutral hydrogen (H I) λ21 cm absorption detected towards the arcsecond-scale radio jet of the Seyfert 1.5 galaxy Markarian 6. Absorption is detected only towards a bright, compact radio feature located, in projection, ~ 380 pc north of the likely location of the optical nucleus. Based on comparison with an archival HST image, we propose a geometry in which the H I absorption arises in a dust lane passing north of, but not covering, the optical nucleus, and the southern lobe of the jet is oriented on the near side of the inclined galaxian disk. We note that this result is contrary to previous models which place the extended narrow-line region on the near side of the disc.

Key words: galaxies: active – galaxies: jets – galaxies: kinematics and dynamics – galaxies: Seyfert – galaxies: individual: Markarian 6

1. Introduction

Emission from hot, ionised gas distinguishes active galactic nuclei (AGNs) from quiescent galaxies. However, conventional models for AGNs depend on the distribution and kinematics of colder, neutral media. Firstly, the host galaxy is a massive reservoir of neutral gas which might ultimately feed an energetic accretion disc, although the means by which gas funnels down to sub-parsec scales in not well understood (Rees 1984). Secondly, the unifying schemes for AGNs propose that the apparent differences between broad-line AGNs (i.e. Seyfert 1s) and narrow-line AGNs (Seyfert 2s) result from selective obscuration through neutral, dusty gas located along the sight-line to the broad-line region (Antonucci & Miller 1985).

Exploring the neutral gas in AGNs is challenging because the surface brightness of emission is generally too faint to detect on scales much smaller than $\sim 1''$. We are instead continuing a programme to explore neutral hydrogen (H I) in *absorption* towards AGNs with the goal of establishing the distribution and kinematics on scales as small as $0\farcs1$, or roughly 10 parsecs in the nearest Seyfert galaxies (Pedlar et al. 1995; Mundell et al. 1995; Gallimore et al. 1994). In this work, we present MERLIN observations of 21 cm absorption towards the Seyfert 1.5 nucleus of Mkn 6. The localisation of the H I absorption suggests a particular alignment between the host galaxy disc and the radio jet. After first describing the observations and results, we discuss the implications of this alignment in further detail. For comparison with earlier papers, we adopt a distance of 77 Mpc to Mkn 6, appropriate for $H_0 = 75$ km s^{-1} Mpc^{-1}, and giving a scale of $1''$= 374 pc (Meaburn et al. 1989).

Send offprint requests to: J.F. Gallimore

2. Observations

We observed Mkn 6 with the 8-element MERLIN array (Wilkinson 1992), including the Lovell telescope; the results are summarised in Fig. 1. The observations were tuned to the 1420 MHz hyperfine transition of H I centered near the Doppler velocity $cz = 5800$ km s^{-1} (heliocentric, optical convention). The systemic velocity of the host galaxy is actually 5640 ± 10 km s^{-1} (Meaburn et al. 1989), well within the observed bandwidth. The velocity resolution of the observations is 26.4 km s^{-1}, and, after removing end channels with poor frequency response, the effective bandwidth is $\sim$6.6 MHz (1400 km s^{-1}).

Data reduction followed standard techniques employed for MERLIN data, including initial calibration and processing with software local to Jodrell Bank. Further data processing, including self-calibration against line-free continuum channels, was performed within the AIPS data reduction package. Channel maps and line-free continuum images were produced following standard numerical Fourier transform techniques and deconvolution using the CLEAN algorithm (Högbom 1974). A more detailed description of the MERLIN data reduction techniques employed can be found in Mundell et al. (1995).

We constructed both naturally and uniformly weighted spectral line cubes. Continuum images were generated by averaging over channels with no significant line detections. For the naturally weighted images, the restoring beam dimensions (FWHM) are $0\farcs32 \times 0\farcs27$, P.A. -21°, and the respective continuum and spectral line sensitivities are 0.13 mJy beam^{-1} and 0.68 mJy beam^{-1} (1σ). The resolution of the uniformly weighted images

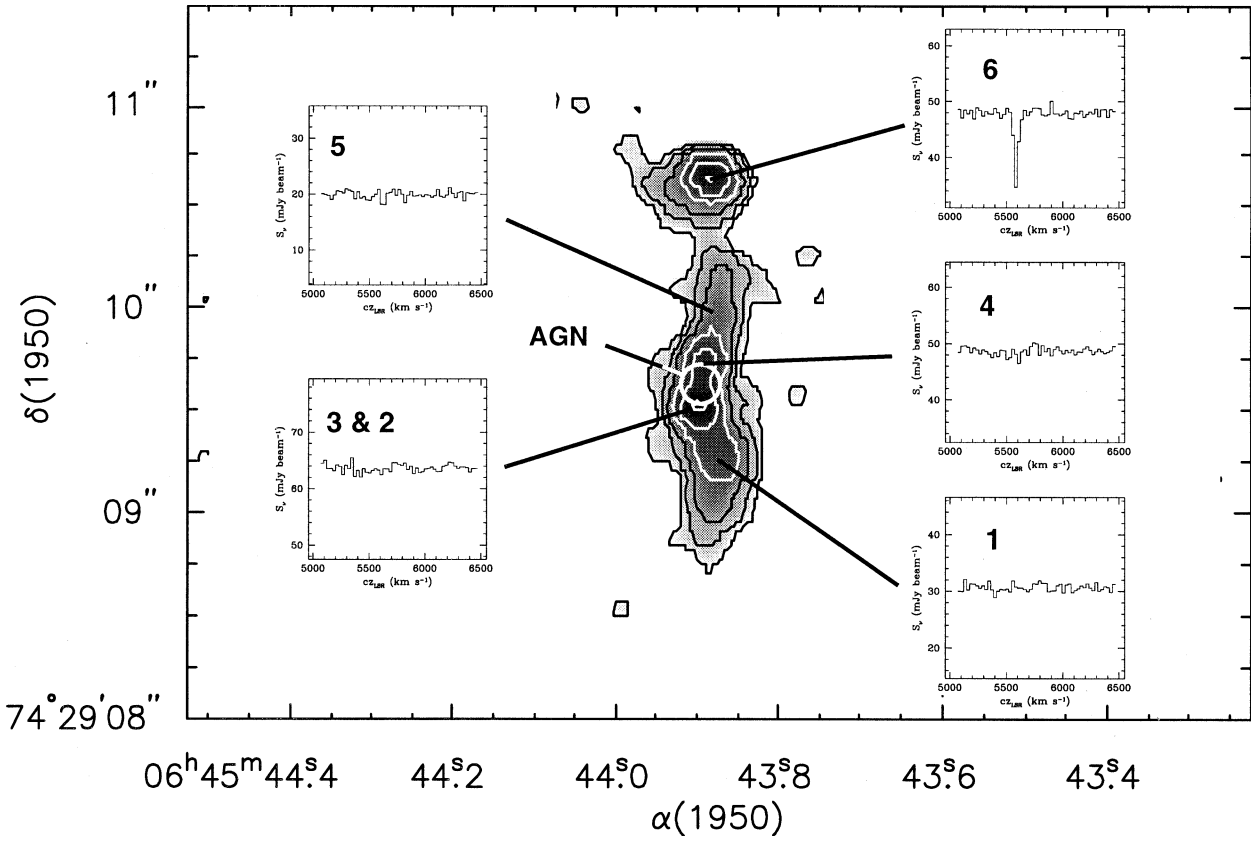

Fig. 1. Results of the H I absorption experiment. The uniformly weighted, 21 cm continuum image is displayed as contours over greyscale. The white circle indicates the location of the AGN according to the alignment of Capetti et al. (1995). The naturally weighted spectra towards each bright component of the radio jet are displayed as overlays. H I absorption is clearly detected towards component 6, but a search over the data cube reveals no other significant absorption. The continuum contour levels, in mJy beam^{-1}, are: ± 0.53 (3σ), 1.2, 2.9, 6.8, 15.9, and 37.3 (logarithmic scaling). The restoring beam dimensions are: natural weight, $0\farcs32 \times 0\farcs27$, P.A. -21°; and uniform weight, $0\farcs16 \times 0\farcs14$, P.A. 88°.

is $0\farcs16 \times 0\farcs14$, P.A. 88°, and the continuum and spectral line sensitivities are 0.19 mJy beam^{-1} and 1.2 mJy beam^{-1}.

3. Results

In contrast to the radio continuum emission from Mkn 6, which is extended and highly structured (e.g., Kukula et al. 1996; Fig. 1), H I absorption is detected only towards component 6, a compact source located at the northern end of the arcsecond-scale radio jet (Fig 1; component numbering following Kukula et al. 1996). Discussed further below, the linewidth is very narrow in comparison with H I absorbed radio jets in other Seyfert galaxies; formally, the linewidth (FWHM) is 33 ± 6 km s^{-1} (corrected for the instrumental resolution) and the maximum opacity is $\tau_{max} = 0.45 \pm 0.01$. The integrated absorption profile corresponds to a foreground column of

$$N_{HI} = (2.6 \pm 0.3) \times 10^{21}\ (T_S/100\ \mathrm{K})\ \mathrm{cm}^{-2}\ ,$$

where T_S is the spin (excitation) temperature of the ground state. This column is not unusual for a sight-line through an inclined disk galaxy. However, we note that a similar column, detected in NGC 4151, was interpreted as absorption in a nuclear torus (Mundell et al. 1995).

The limits placed by non-detections better define the localisation of the H I absorption around component 6. Towards the brighter regions of the southern jet, components 2–4, the (3σ) limit is $\tau_\nu \lesssim 0.07$, corresponding to a foreground column density

$$N_{HI} \lesssim 4 \times 10^{20}\ \mathrm{cm}^{-2}\ (T_s/100)(\Delta v/30\ \mathrm{km\ s}^{-1})\ .$$

The absorbing gas would easily have been detected had the gas completely covered the jet. On the other hand, component 5, which is the nearest neighbor to the absorbed component, is much fainter, and so the limits are less stringent: $\tau_\nu \lesssim 0.9$, or

$$N_{HI} \lesssim 5 \times 10^{21}\ \mathrm{cm}^{-2}\ (T_s/100)(\Delta v/30\ \mathrm{km\ s}^{-1})\ .$$

We can conclude is that the H I absorbing gas covers a region including component 6 and extending no further south than component 5, or roughly $0\farcs75$ (280 pc in projection). However, we can place no limits on the extent of the absorbing gas in other directions.

The centroid velocity of the absorption line is 5584 ± 3 km s^{-1}, blue-shifted relative to systemic by 56 ± 10 km s^{-1}. For comparison, the position-velocity curve is plotted in Fig. 2. The details of the rotation curve within the inner few arcseconds are

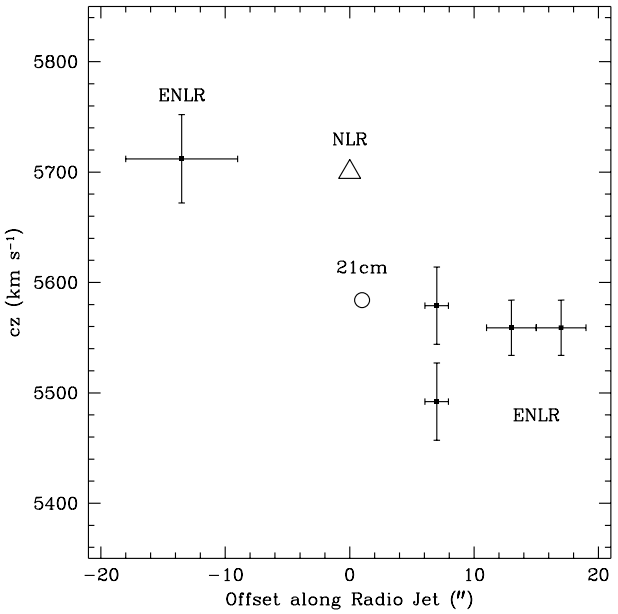

Fig. 2. The location of the H I absorption line (open circle) on the position-velocity diagram for Mkn 6. The centroid velocities of the extended narrow line region (ENLR; filled squares) and NLR (open triangle) are taken from Meaburn et al. (1989). The ENLR traces kinematically quiescent gas that is exposed to the AGN, and so defines the inner rotation curve. Within the errorbars, the H I absorption is located roughly where expected on the rotation curve, and so probably arises from gas in normal rotation about the galaxy center.

unknown, but the velocity of the 21 cm absorption line does not appear significantly displaced from any plausible rotation curve. We conclude that the absorption line arises in otherwise normally rotating gas, and there is no evidence for streaming motions greater than ~ 50 km s^{-1}. Furthermore, we do not detect any velocity gradients across component 6. Assuming that the absorbing gas completely covers the background source (Sect. 4), the upper limit for the velocity gradient is approximately the width of the absorption line divided by the component size ($\sim 0\farcs08$; Kukula et al. 1996), or < 1.0 km s^{-1} pc^{-1}. For comparison, the projected velocity gradient of the H I absorption seen towards NGC 4151 is ~ 3 km s^{-1} pc^{-1} (Mundell et al. 1995).

4. Discussion

The trivial explanation for the localised H I absorption is an isolated cloud which fortuitously aligns with component 6. We consider it more likely, however, that the absorbing gas lies in the galaxy disk surrounding the nucleus. For example, this result compares favorably with the localised H I absorption observed towards the radio jet of NGC 4151 (Mundell et al. 1995). The interesting question is whether, as was proposed for NGC 4151, the absorbing gas might be located in small-scale ($\lesssim 100$ pc) disc surrounding the AGN. In the case of Mkn 6, however, we find that absorption from gas distributed on kpc-scales is more consistent with the observations. The first evidence is that the linewidth is very narrow, ~ 30 km s^{-1}, which is less than half the H I absorption linewidth of NGC 4151. In contrast, H I absorption linewidths towards Seyfert and starburst galaxies often exceed 100 km s^{-1}, particularly in those cases where the H I absorption is known to trace gas deep in the nucleus (Pedlar et al. 1996; Mundell et al. 1995; Gallimore et al. 1994; Dickey 1986). This evidence is not sufficient, however, since we cannot rule out the possibility that the absorption arises from a compact, circularly rotating disc viewed nearly face-on. Nevertheless, the narrowness of the line is consistent with that expected from a larger scale ring or disc.

We next examine the displacement of the absorption from the AGN. Unfortunately, the correspondence between components in the optical and radio images is not accurately known. Moreover, the continuum spectra and sizes of the radio features are indistinct, and so there is currently no clear radio candidate for the AGN proper (Kukula et al. 1996). Clements (1983) places the optical nucleus somewhere between component 5 and (the H I absorbed) component 6, but the uncertainties are roughly one quarter the length of the radio jet. Nevertheless, the Clements position is significantly displaced southward from component 6 (Kukula et al. 1996). Capetti et al. (1995) propose an alignment between the radio and optical images based on *Hubble Space Telescope* images. They found a linear extension of [O III] emission that agrees well both in orientation and detailed shape with the southern part of the radio jet (i.e., components 1–5). Aligning the radio and optical jet structures places the AGN $\sim 1''$ (~ 380 pc in projection) south of component 6, somewhere nearer component 3 (from Kukula et al.: $\alpha_{(J2000)} = 6^h\ 52^m\ 12\fs336$, $\delta_{(J2000)} = 74^\circ\ 25'\ 37\farcs08$; $S_\nu(20\ \mathrm{cm}) = 16$ mJy). Adopting this alignment, and further considering the narrowness of the absorption line, we are drawn to the conclusion that the H I absorption in Mkn 6 arises from neutral gas displaced from the nucleus by $\gtrsim 400$ pc. For reference, the strongest absorption lines observed towards the Seyfert nucleus of NGC 1068 similarly trace a ~ 500 pc radius, central disc (Gallimore et al. 1994).

From a more detailed study of the optical and radio continuum structures of the nucleus (Holloway et al. in preparation), we have discovered a conspicuous candidate for the H I absorber. Illustrated in Fig. 3, there is an obvious band of increased extinction which crosses $\sim 1''$ north of the optical nucleus. For convenience, we refer to this dark region simply as a dust lane. According to the alignment of Capetti et al. (1995), the dust lane encompasses the position of the H I absorbed radio feature. The high aspect ratio of the dust lane suggests a disk or spiral arms viewed edge-on.

The simplest picture is that the dust lane traces a kpc-scale disc or ring surrounding the nucleus, or perhaps a spiral arm segment lying in front of the nucleus. The radio jet must be oriented with component 6 lying behind the disc to the north and components 1–5 in front of the disc to the south. There are two important implications of this result. Firstly, the location of the H I absorbed radio feature within the newly discovered dust lane lends self-consistent support for the Capetti et al. alignment, which, as a corollary, strengthens their argument for an interaction between the radio jet and the NLR gas. The sec-

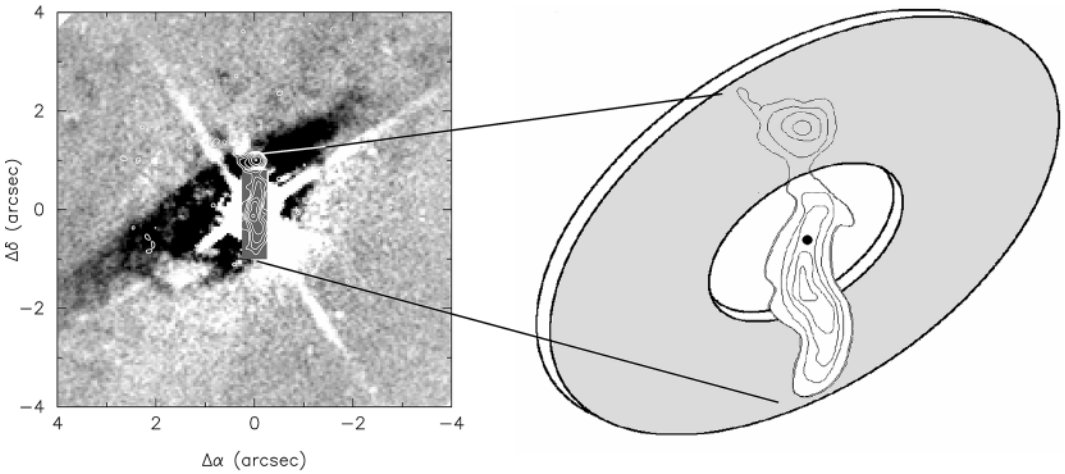

Fig. 3. Illustration of the H I absorbing medium of Mkn 6. The *left panel* is an overlay of the 21 cm radio continuum and an archival HST image taken in the F606W (wide V-band) filter. We have subtracted an elliptical isophote model of the smooth, bulge light from the HST image in order to enhance the contrast of the underlying structure. The halftone rendering of the HST image is displayed in the positive sense: the dark band across the nucleus is an apparent band of high extinction, presumably arising in a dust lane. We chose the Capetti et al. (1995) alignment between the MERLIN and HST images. Only component 6 among the brighter jet features lies, in projection, within the dust lane. The cartoon in the *right panel* depicts a plausible ring geometry for the neutral, absorbing gas. The proposed location of the AGN, near radio component 3, is indicated by the dot. This cartoon is purely illustrative and is not intended to be a detailed model for the MERLIN H I absorption and HST data.

ond implication is that the northern jet and NLR structures fall behind the galaxian disc, contrary to our earlier model for the northern ionisation cone (Kukula et al. 1996). More specifically, there is a strong correspondence between [O III] emission and radio emission only at the southern end of the jet. The lack of [O III] emission towards the northern end of the jet (i.e., component 6) is naturally explained by extinction in our model for the H I absorption. We will explore a revised model for the ionisation cone structure in a follow-up paper (Holloway et al. 1997).

5. Conclusions

Our primary results and conclusions are as follows.

1. There is no H I absorption detected toward the probable location of the AGN of Mkn 6. This result is consistent with the more general picture that sight-lines towards Seyfert 1 nuclei are relatively unobscured.
2. The detected H I absorption probably arises from a kpc-scale distribution of gas, possibly a disc, spiral arms, or a ring, surrounding the nucleus and associated with a conspicuous dust lane passing north of the AGN.
3. The kinematics of the H I absorption line gas places it near the systemic velocity as interpolated from measurements of the ENLR. Unlike other H I absorbed Seyfert nuclei (Dickey 1986), there is no evidence for rapid streaming motions in the absorbing gas.
4. The radio jet is probably oriented behind the galactic disc to the north and in front of the galactic disk to the south. If, as appears to be the case for most Seyfert nuclei, the NLR and ENLR gas share a similar axis with the radio jet, this result places the northern ENLR on the far side of the disc, contrary to earlier models.

Acknowledgements. J.F.G. received collaborative travel support from the University of Manchester Dept. of Astronomy and computer support at NRAL, Jodrell Bank during the completion of this work. C.G.M. acknowledges receipt of a PPARC Research Fellowship.

References

Antonucci R.R.J., Miller J.S., 1985, ApJ 297, 621
Capetti A., Axon D.J., Kukula M., et al., 1995, ApJ 454, L85.
Clements, E.D., 1983, MNRAS, 204, 811
Dickey J.M., 1986, ApJ 300, 190
Gallimore J.F., Baum S.A., O'Dea C.P., Brinks, E., Pedlar, A., 1994, ApJ 422, L13
Högbom J.A., 1974, A&AS 15, 47
Kukula M.J., Holloway A.J., Pedlar A., et al., 1996, MNRAS 280, 1283
Meaburn J., Whitehead M.J., Pedlar A., 1989, MNRAS 241, 1p
Mundell C.G., Pedlar A., Baum S.A., et al., 1995, MNRAS 272, 355
Pedlar A., Mundell C.G., Gallimore J.F., Baum S.A., O'Dea C.P. 1995, VA 40, 91
Rees M.J., 1984, ARA&A 22, 471
Wilkinson P.N., 1992, in: Subarcsecond Radio Astronomy, eds. Davis R.J., Booth R.S., Cambridge Univ. Press, Cambridge, p. 422